

Novel Donor-acceptor Type Electrochromic Polymers based on [1,2,5]thiadiazolo[3,4-c] pyridine as the acceptor unit

Xiaoli Liu^{1,2}, Lingqian Kong³, Yan Zhang², Xiuping Ju³, Jinsheng Zhao^{2,*}, Yanhong Li^{1,*}

¹Shool of materials Science and Engineering, Shenyang university of Chemical Technology, Shenyang, 110142, P. R. China

²Shandong Key Laboratory of Chemical Energy Storage and Novel Cell Technology, Liaocheng University, Liaocheng, 252059, P.R. China

³Dongchang College, Liaocheng University, Liaocheng, 252059, P. R. China

*E-mail: j.s.zhao@163.com (j.s.zhao); lyhciem@126.com (Y.H.Li)

Received: 4 October 2015 / Accepted: 7 November 2015 / Published: 1 December 2015

Three novel donor-acceptor type π -conjugated polymers, Poly[4,7-bis(2,3-dihydrothieno[3,4-b][1,4]dioxin-5-yl)-[1,2,5]thiadiazolo[3,4-c]pyridine] (PEDOT-PT), Poly[4,7-bis(4-methylthiophen-2-yl)-[1,2,5]thiadiazolo[3,4c] pyridine] (PMTTP) and Poly[4, 7-bis(4-butylthiophen-2-yl)-[1,2,5]thiadiazolo[3,4-c] pyridine] (PBTTP) containing [1,2,5]Thiadiazolo[3,4-c]pyridine (PT) unit in the skeleton as the acceptor unit and variable thiophene derivatives as the donor units are obtained by electrochemical polymerization method. For investigating their electrochemical and electrochromic nature, the polymers were evaluated by cyclic voltammetry (CV), UV-vis spectroscopy, step profiler, and scanning electron microscopy (SEM). PEDOT-PT with strong electron-donating EDOT group has lower oxidation potential than that of PMTTP and PBTTP. The band gap of polymers were evaluated according to the spectroelectrochemistry analysis, and were 0.85 eV, 1.31 and 1.46 eV for PEDOT-PT, PMTTP and PBTTP, respectively. Electrochromic investigations showed that the polymers having variable electron-donating groups exhibit different electrochromic performance, including variable colors, switching potential difference and the changes in transmittances. PEDOT-PT showed reversible redox switches accompanied by color variance from its blue-green neutral state to blue fully oxidized state. PMTTP switches between dark blue and light blue and PBTTP changes between bluish violet to grey. Besides, all of the polymers showed impressive kinetic quality, including more than 60% optical changes in the NIR region and high coloration efficiencies and short response times which make the polymers predominant candidates for electrochromic usages.

Keywords: [1,2,5]Thiadiazolo[3,4-c]pyridine (PT); lower band gap; satisfactory coloration efficiencies

1. INTRODUCTION

Conjugated polymers have become arresting since it was discovered with the potential use as the functional layers in series appliance [1]. Along with continuous renewal of the molecular frameworks of the polymers, application fields have been broadened to new areas including photovoltaic devices[1], light-emitting diodes (LEDs)[2], field effect transistors[3], sensors[4], and electrochromic devices[5]. The use of conjugated polymers as active layers in electrochromic devices has received enormous attention because of their high optical contrasts [6], fast switching times[7], processability, and fine-tuning of the band gap by structure modification[8]. Up to date, types of electrochromic devices have been designed including smart windows, rear-view mirrors for cars and electrochromic displays. First introduced in the early 1990's by Havinga et al., the "donor-acceptor" means characterized with alternate electron-rich and electron-deficient moieties along the chain framework of the polymer has been shown applicable to obtain dual-band and broadly absorbing polymer chromophores with photovoltaic and/or electrochromic properties [9,10]. The use of fused aromatics with electron-withdrawing imine nitrogens (C=N) as acceptor units and different thiophene derivatives as donor units has drawn great interest to design these alternating systems.

It has been reported that several acceptor units, such as benzothiadiazole[11], benzotriazole[12], quinoxaline[13], diketopyrrolopyrrole[14], pyrido[3,4-b]pyrazine[15], and thieno[3,4-c]pyrrole-4,6-dione[16], have displayed several advantages involving red-shifting of absorption band, and improvement of the electrochromic properties. [1,2,5]Thiadiazolo[3,4-c]pyridine (PT), with the only molecular difference of nitrogen atom on the pyridine ring from benzothiadiazole (BT), has a higher electron affinity than that of BT. The PT hetero cycle has been employed as an electron-deficient unit in the synthesis of the polymer photovoltaic materials and panchromatic organic sensitizers for Dye-sensitized mesoscopic solar cells[17,18]. It is notable that, in 2011, Heeger and his co-workers reported the highest conversion efficiency of 6.7% for solution-processed small molecular solar cells of that time by incorporating PT as the acceptor unit inside the small molecule, indicating that PT is a promising electron acceptor unit[19]. Besides, we previously reported the synthesis of PMOTTP and PBOTTP containing strong electron-accepting PT as acceptor unit. Both PMOTTP and PBOTTP can present red, green, and blue (RGB) display in one polymer, and be considered as interesting candidates for electrochromic materials.

Recently, the polymer Poly (4,7-bis(2,3-dihydrothieno[3,4-b][1,4]dioxin-5-yl)-[1,2,5]thiadiazolo [3,4-c] pyridine) (EDOT-PT) containing alternating bi-EDOT as the donor unit and PT as the acceptor unit was synthesized by Xu et al., and its thermoelectric performance was investigated in detail [20].

In order to study the electrochromic properties of the poly (EDOT-PT) polymer along with the effects of the electron-rich units on the characteristics of the polymers, three monomers including 4,7-bis(2,3-dihydrothieno[3,4-b][1,4]dioxin-5-yl)-[1,2,5]thiadiazolo[3,4-c]pyridine (EDOT-PT), 4,7-bis(4-methylthiophen-2-yl)-[1,2,5]thiadiazolo[3,4-c]pyridine (MTTP) and 4,7-bis(4-butylthiophen-2-yl)-[1,2,5]thiadiazolo[3,4-c]pyridine (BTTP) were synthesized. The corresponding polymers have been prepared by the electropolymerization method and their specific characteristics concerning the electrochromic performance has been studied in detail. The electrochemical properties, optical

properties electrochromic switching properties were studied. Effects of the different donor unit on electrochemical and spectral behavior of the obtained polymers were also discussed in detail.

2. EXPERIMENTAL

2.1 General

2,5-dibromopyridine-3,4-diamine [21,22], 4,7-dibromo-[1,2,5]thiadiazolo[3,4-c]pyridine and tributylstannane compounds were prepared according to the literature method [23]. ^1H NMR and ^{13}C NMR spectroscopy studies were carried out on a Varian AMX 400 spectrometer and the chemical shifts (δ) were given relative to tetramethylsilane as the internal standard. Electrochemical synthesis and experiments were performed in a one-compartment cell with a CHI 760 C Electrochemical Analyzer controlled by a computer, employing a platinum wire with a diameter of 0.5 mm as working electrode, a platinum ring as counter electrode, and a Ag wire (0.02 V vs. SCE.) as pseudo-reference electrode. Before and after each experiment, the silver pseudo reference was calibrated versus the ferrocene redox couple and then adjusted to match the SCE reference potential. Electrodeposition was conducted in a 0.2 M solution of tetrabutylammonium hexafluorophosphate (TBAPF_6) at scan rate of 100 mVs^{-1} for 10 cycles. Scanning electron microscopy (SEM) measurements were taken by using a Hitachi SU-70 thermionic field emission SEM. The thickness and surface roughness of polymer films were carried on KLA-Tencor D-100 step profiler. UV-Vis-NIR spectra were recorded on a Varian Cary 5000 spectrophotometer connected to a computer. A three-electrode cell assembly was used for spectroelectrochemistry measurement where the working electrode was an indium tin oxide (ITO) glass, the counter electrode was a stainless steel wire, and an Ag wire was used as pseudo reference electrode. The polymer films for spectroelectrochemistry were prepared by potentiostatically deposition on ITO glass slides (the active area: $1.0 \text{ cm} \times 2.8 \text{ cm}$). The thickness of the polymer films grown potentiostatically on ITO was controlled by the total charge passed through the cell and was measured by step profiler. Digital photographs of the polymer films were taken by a Canon Power Shot A3000 IS digital camera [24].

2.2 Synthesis procedure

2.2.1 2,5-dibromopyridine-3,4-diamine

The mixture of pyrido-3,4-diamine (2 g, 18.3 mmol) with an aqueous HBr (48%, 30 ml) were prepared in a 250 ml three-neck round-bottom flask with a magneton inside. After the mixture was heated to $100 \text{ }^\circ\text{C}$, bromine (2.5 ml) was added dropwise, and the solution was stirred for 5 h at $135 \text{ }^\circ\text{C}$. The mixture was cooled to room temperature, an aqueous solution of $\text{Na}_2\text{S}_2\text{O}_3$, an aqueous solution of Na_2CO_3 , and distilled water were added in this order to get a yellow precipitate. Then the precipitate was separated by filtration and washed by distilled water three times. Recrystallization from the mixture solution of toluene:THF (v:v=5:1) gave white flocculence of 3,4-diamino-2,5-dibromopyridine (yield = 51%). ^1H NMR (400MHz, DMSO, δ): 7.53 (s, 1H), 5.99 (s, 2H), 5.03 (s, 2H). ^{13}C NMR (100 MHz, CDCl_3 , δ): 139.93, 139.13, 129.54, 126.67, 106.22 [25].

2.2.2 4,7-dibromo-[1,2,5]thiadiazolo[3,4-c]pyridine

To a 100 ml three-neck round bottom flask equipped with a magnetic stirring bar, 2,5-dibromopyridine-3,4-diamine (1.1 g, 3.8 mmol) and pyridine (12 mL) were added successively under nitrogen atmosphere. The SOCl_2 (0.7 mL) was then dropped, the resulting mixture was stirring at 0 °C until a deep pink colored solution was obtained. This was followed by reflux at 80 °C overnight. The reaction mixture was allowed to cool to room temperature. The reaction mixture was filtered and washed with water repeatedly, dried over anhydrous MgSO_4 [24]. The crude mixture was chromatographed on silica gel by eluting with hexane/ dichloromethane (4:1, v/v) to give the yellow solid. ^1H NMR (300 MHz, CDCl_3 , δ): 8.552 (s, 1H). ^{13}C NMR (100 MHz, CDCl_3 , δ): 162.79, 160.88, 153.17, 139.18, 96.22.

2.2.3 General procedure for the synthesis of MTTP, BTTP and EDOT-PT via Stille Coupling

4,7-dibromo-[1,2,5]thiadiazolo[3,4-c]pyridine (1.00 g, 3.4 mmol), and the excessive tributyl(4-methylthiophen-2-yl)stannane (17 mmol), tributyl(4-butylthiophen-2-yl)stannane (17 mmol) or tributyl(2,3-dihydrothieno[3,4-b][1,4]dioxin-5-yl)stannane (17 mmol) using $\text{Pd}(\text{PPh}_3)_2\text{Cl}_2$ (0.238 g, 0.34 mmol) as the catalyst were dissolved in anhydrous toluene (80 mL) at room temperature. The solution was stirred under nitrogen atmosphere for 30 min. Raise the temperature immediately until the solution was refluxed. The mixture was stirred under nitrogen atmosphere for 24 h, cooled and concentrated on the rotary evaporator. Lastly the residue was purified by column chromatography on silica gel using hexane-dichloromethane (1:1, v/v) as the eluent.

2.2.4 4,7-bis(4-methylthiophen-2-yl)-[1,2,5]thiadiazolo[3,4c]pyridine (MTTP)

The crude mixture was chromatographed on silica gel by eluting with hexane: dichloromethane (1:2, v/v) to give MTTP as red solid (0.8 g, 69%). ^1H NMR (400 MHz, CDCl_3 , δ /ppm): 8.75, 8.45, 7.99, 7.16, 7.04, 2.36. ^{13}C NMR (100 MHz, CDCl_3 , δ /ppm): 155.07, 149.21, 145.50, 141.58, 140.97, 139.74, 139.03, 136.49, 134.11, 130.35, 126.51, 122.97, 120.64, 16.09 [24].

2.2.5 4,7-bis(4-butylthiophen-2-yl)-[1,2,5]thiadiazolo[3,4-c]pyridine (BTTP)

The crude mixture was chromatographed on silica gel by eluting with hexane: dichloromethane (1:3, v/v) to give BTTP as red solid (0.74 g, 54%). ^1H NMR (400 MHz, CDCl_3 , δ /ppm): 8.77, 8.50, 7.94, 7.18, 7.06, 2.70, 1.70, 1.43, 0.97. ^{13}C NMR (100 MHz, CDCl_3 , δ /ppm): 155.07, 149.22, 146.52, 145.39, 144.57, 141.54, 140.95, 136.43, 133.26, 129.54, 125.96, 122.15, 120.69, 32.96, 30.54, 22.64, 14.17[30].

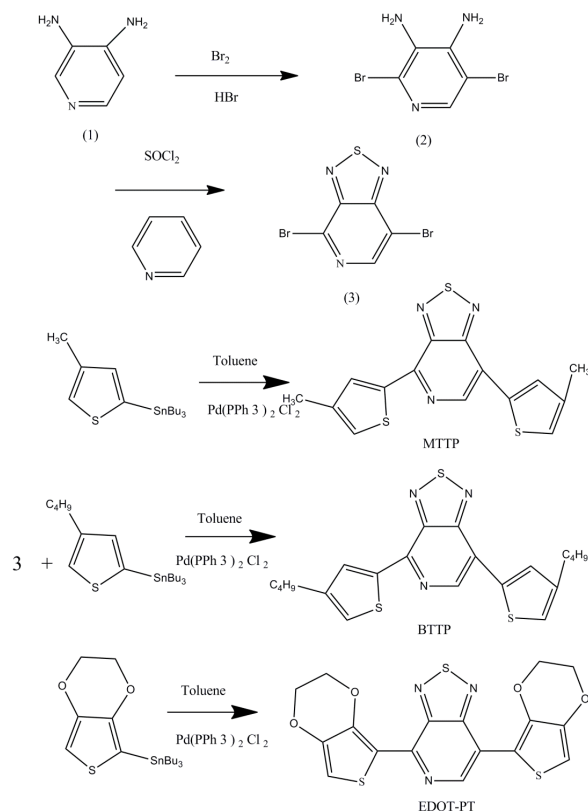
2.2.6. 4,7-bis(2,3-dihydrothieno[3,4-b][1,4]dioxin-5-yl)-[1,2,5]thiadiazolo[3,4-c]pyridine (EDOT-PT)

The crude mixture was chromatographed on silica gel by eluting with hexane: dichloromethane (1:3, v/v) to give ETTP as dark red solid (0.78 g, 51%). ^1H NMR (400 MHz, CDCl_3 , δ /ppm): 9.45, 6.72, 6.59, 4.49, 4.35. ^{13}C NMR (100 MHz, CDCl_3 , δ /ppm): 154.49, 149.49, 145.69, 143.26, 142.25, 141.99, 140.94, 119.99, 111.65, 106.06, 102.85, 65.66, 64.54.

3. RESULT AND DISCUSSION

3.1 Synthesis of monomers

The synthesis of monomer of MTTP BTTP and EDOT-PT was carried out with slight modifications of the well-established literature procedures (Scheme 1). The first step of this route involved the bromination of pyridine-3,4-diamine in the presence of HBr/Br_2 mixture. The second step, 4,7-dibromo-[1,2,5]thiadiazolo[3,4-c]pyridine was given through oxidation with an excess amount of SOCl_2 in pyridine solvent. The organotin compound was synthesized follow previously literature[24]. The last step, the Stille coupling reaction was achieved in anhydrous toluene in the presence of a catalytic amount of $\text{Pd}(\text{PPh}_3)_2\text{Cl}_2$. The reactions proceeded quite nicely to afford MTTP BTTP and EDOT-PT with satisfactory yields.



Scheme 1. Synthetic route of the monomers.

3.2 Electrochemical polymerization

The polymerization of the monomers are conducted by the CV method. All polymers were deposited on the working electrode (Pt wire) by CV with the same scan rate (100 mV s^{-1}) in acetonitrile (ACN)/dichloromethane (DCM) (1:1, by volume) solvent mixture containing 0.2 M tetrabutylammonium hexafluorophosphate (TBAPF_6) as the supporting electrolyte and 0.005 M monomers. The CV curves for the electrodeposition of three monomers were shown in Fig.1. The first cycle of the CV test ascribed oxidation of monomer and the onset oxidation potentials (E_{onset}) of EDOT-PT is 0.94 V. The E_{onset} values of MTTP and BTTP are 1.32 V and 1.28 V, respectively[24]. As can be seen in Figure 1, fairly well-defined redox waves are found for the polymerization of the monomer EDOT-PT, with the oxidation peak ($E_{\text{p,ox}}$) at 0.68 V and the reduction peak ($E_{\text{p,red}}$) at 0.51 V. The values of the redox peaks are 1.07 V ($E_{\text{p,ox}}$) and 0.89 V ($E_{\text{p,red}}$) for MTTP, 0.90 ($E_{\text{p,ox}}$) and 0.82 V ($E_{\text{p,red}}$) for BTTP respectively. With the increase of the number of CV scans, the amplitudes of the electric currents increase, indicating the formation of redox polymer at the working electrode surface. The broad CV curves as shown in Fig.1 might be an indication of the polydispersity of the molecular weight of as-formed polymer, and also could be caused by the conversion of conductive species on polymer main [26]. By contrast, the oxidation potential of EDOT-PT was the lowest in all of three monomers, since the electron donating effect of EDOT-PT was the strongest and EDOT-PT had a more effect D-A match than other monomers.

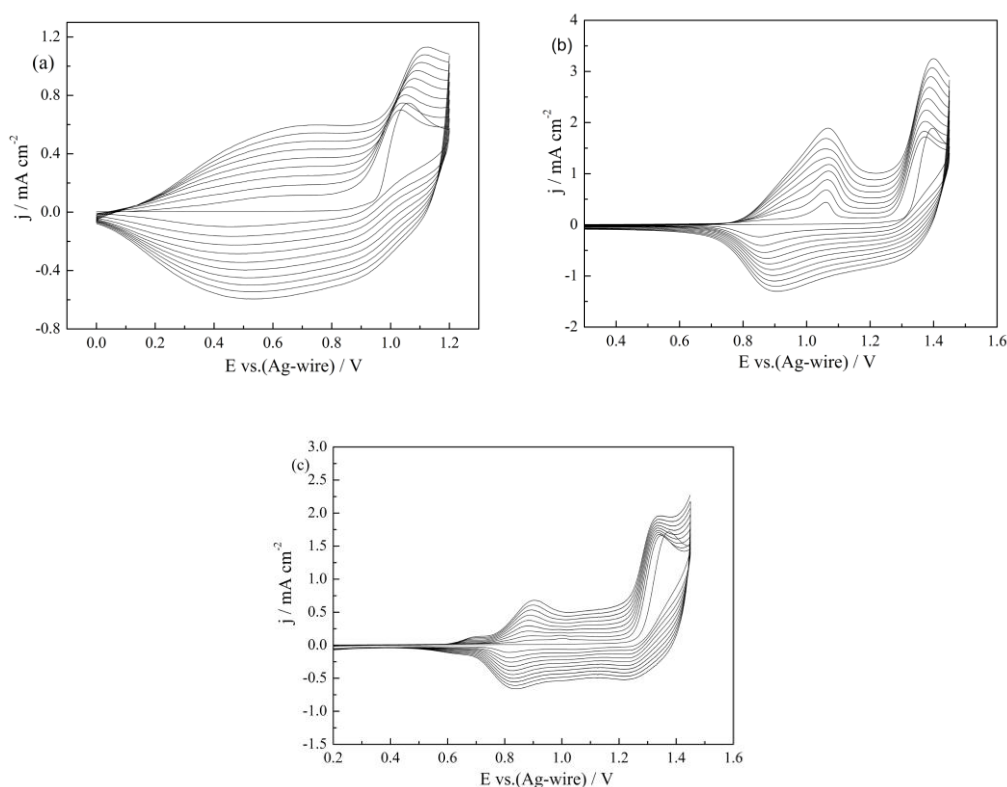


Figure 1. Cyclic voltammogram curves of EDOT-PT(a), MTTP(b) and BTTP (C) in ACN/DCM(1:1) containing 0.2 M TBAPF_6 solutions at a scan rate of 100 mV s^{-1} .

In order to get a information about the redox activities of the polymer films, the CV of the as-prepared polymer film on the Pt wire (electropolymerized by three cycles) was conducted in the electrolyte solution with the absence of monomers at different scan rates between 25 and 300 mV s^{-1} . The CV curves of PEDOT-PT polymer was demonstrated at Fig.2a. A pair of redox peaks were clearly observed with an oxidation peak and a reduction peak located at 0.51 V and 0.53 V, respectively, in the p-doping process for PEDOT-PT. A pair of redox peaks were located at 0.99 and 0.94 for PMTTP(Fig.2b), 1.14 and 0.95 for PBTTP respectively (Fig.2c). The scan rate dependence of the peak currents density of PEDOT-PT was illustrated in Fig.3. The peak currents were linearly proportional to the scan rates(linear correlation coefficient $R > 0.99$) which indicated a non-diffusional redox process and well-adhered electroactive polymer film [27]. The other two polymers followed the same behavior as that of the PEDOT-PT and the data was not shown.

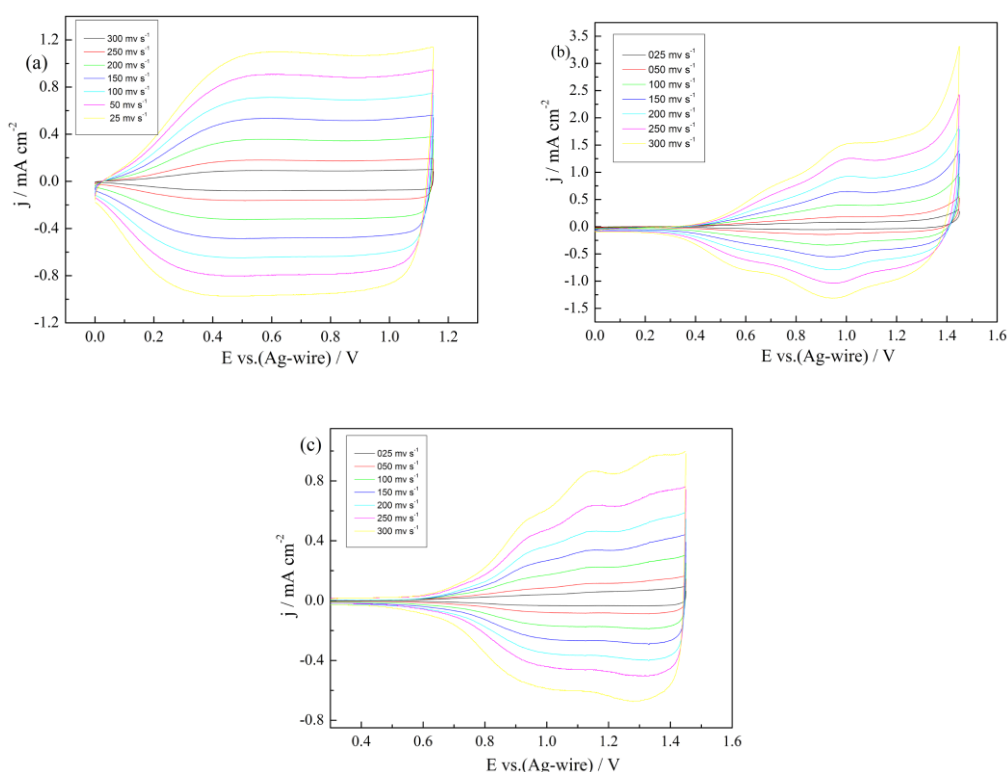


Figure 2. CV curves of the PEDOT-PT (a), PMTTP(b) and PBTTP(c) films at different scan rates between 25 and 300 mV s^{-1} in the monomer-free 0.2 M $\text{TBAPF}_6 / \text{ACN/DCM}$ solution, respectively.

The stability of the active layer materials is of great importance for the application of their industrialization, especially for electrochromic polymers, their long-term cycling stability is an important parameter for consideration[28]. For evaluating the stability performance, the polymer films were electrodeposited on Pt wires by CV method for five cycles as mentioned above, and then its cyclic voltamogram was conducted for 1000 cycles at a scan rate of 200 mV s^{-1} in monomer free electrolyte solution. The overall charge produced in the redox process was calculated for each cycle. As shown in Fig.4, the charge loss for PEDOT-PT was only 3% after 1000 cycles, which indicated that

PEDOT-PT had an extraordinary electrochemical stability. The loss of the total charges were approximately 14% for PMTTP and 12% for PBTP between initial and 1000 th cycle (data was not shown). Since the three compounds have common PT as acceptor, the changes in their stability behaviors are ascribed to the difference of donor. In this study, the stability test was carried out without the exclusion of air, since it is more close to the actual application conditions[24]. We suspected that the charge loss in the stability tests was caused by the catalytic degradation effects of oxygen and water to the deposited polymer film.

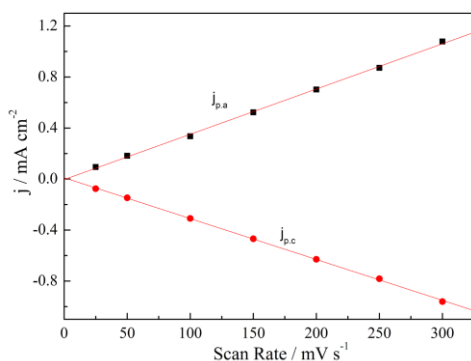


Figure 3. For the PEDOT-PT, the scan rate dependence of the anodic and cathodic peak current densities graph of the p-doping/dedoping process. $j_{p,a}$ and $j_{p,c}$ the anodic and cathodic peak current densities, respectively.

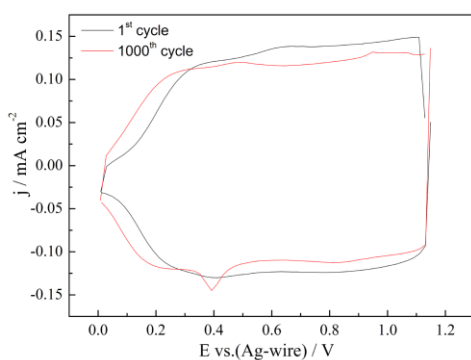


Figure 4. Electrochemical stability of PEDOT-PT in the monomer-free ACN/DCM(1:1) containing 0.2 M TBAPF₆ solutions after 1000 switching by CV method.

3.3. Morphology and thickness

The morphologies of polymer films were closely related with electrochemical properties of polymers. The surface morphologies of three polymers were observed by SEM. The films were prepared by constant potential method in the previously mentioned electrolyte on ITO electrode with the same polymerization charge of 3.0×10^{-2} C and dedoped before characterization. SEM images of these polymer films are clearly shown in Fig.5[24].

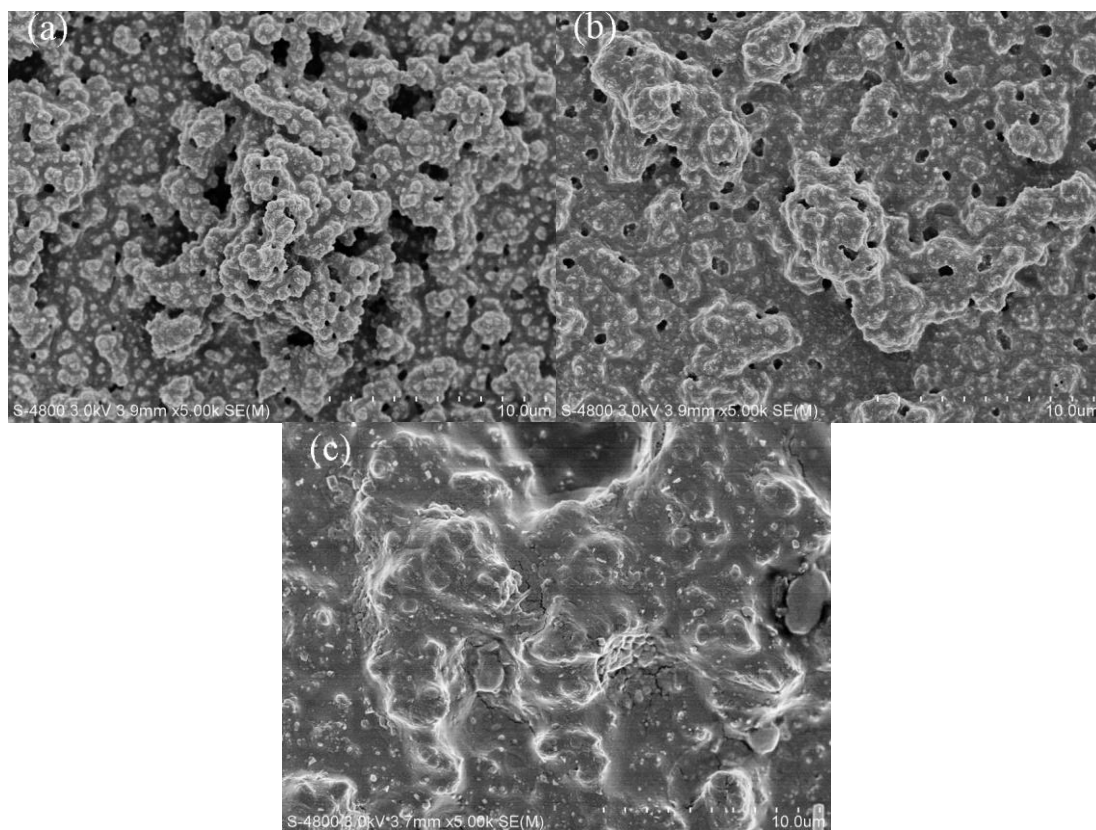
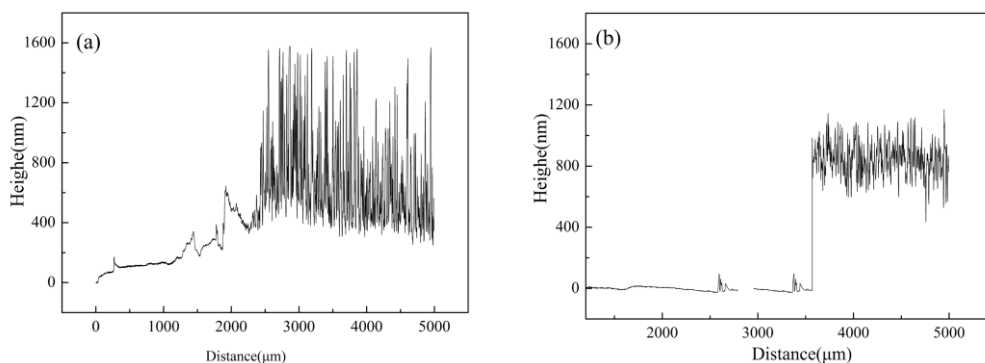


Figure 5. SEM images of (a) PEDOT-PT, (b) PMTTP and(c) PBTTP deposited potentiostatically onto ITO electrode.

The thickness and roughness of three polymer films were investigated by step profiler and these images are shown in Fig.6[24].The thickness of PEDOT-PT, PMTTP and PBTTP was 912 nm, 856 nm, 1011 nm, respectively.This study also revealed that PBTTP had a lowest average roughness value while PEDOT-PT had a highest average roughness value which was consistent with the morphologies given above.The images of step profiler measurements indicated that the polymer films have rough surfaces with detective ditches, which may be advantageous to the doping and dedoping process of the ion to the backbone of the polymers.



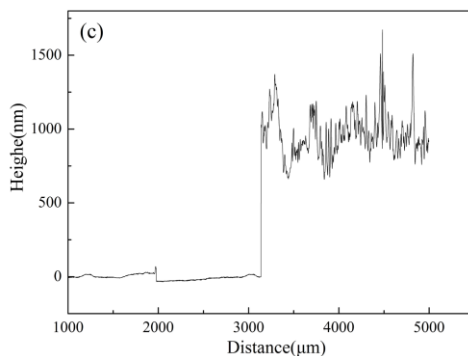


Figure 6. Thicknesses of the PEDOT-PT (a), PMTTP (b) and PBTTP, (c) films deposited potentiostatically onto ITO electrode.

3.4 Optical properties of the monomers and films

Spectroelectrochemical measurements were conducted for obtaining *in situ* optical changes with the increase of the applied potentials. For UV-vis analysis, the monomers are dissolved in CH_2Cl_2 and the polymer films are deposited on ITO electrode and dedoped before analysis, and the data are shown in Fig.7a. All three monomers show two distinct absorption peaks arising from the high energy and the low energy π - π^* transitions, respectively[29]. As seen in Fig. 7a, EDOT-PT has two absorption peaks centered at 315 and 501 nm, respectively. Whereas MTTP revealed a relatively hypsochromic shifted absorption maxima at 305 and 475 nm, respectively, which is similar to that of BTTP. Red shift of the absorption peak of EDOT-PT polymer can be ascribed to the strong electron-donating effect of EDOT group that enhances the conjugation effect and decreases the energy level of π - π^* electronic transition. The optical band gaps (E_g) defined from its low energy absorption edges (λ_{onset}) ($E_g = 1241/\lambda_{\text{onset}}$) are calculated (see Table 1). Not surprisingly when compared the values of E_g , EDOT-PT has the lowest optical gaps which is consistent with the former conclusion. This also further illustrates that EDOT as donor is more matched with PT as acceptor than methyl and butyl as donor.

The UV-vis absorption spectra of the polymer films on the dedoped state were shown in the Fig.7b. Two well-defined absorption peaks centered at 417 and 771nm, and with a valley at about 500 nm was found for PEDOT-PT, which is the typical characteristic of green color film[24]. Table 1 clearly summarizes the maximum absorption wavelength (λ_{max}), the absorption onsets wavelength (λ_{onset}), the optical band gap (E_g), HOMO/LUMO energy levels of the monomers and corresponding polymers. We found that the polymers experienced a red shift in the absorption maximal and low energy absorption edges compared to the corresponding monomers, which was ascribed to the inter chain interaction caused by π -stacking of the polymers[24]. In order to compare with the newly prepared polymers, the parameters of 4,7-bis (2,3-dihydrothieno[3,4-b][1,4]dioxin-7-yl)benzo[c][1,2,5]thiadiazole (PBDT) were also listed in Table 1 [30]. By contrast, the optical band gap of PEDOT-PT is somewhat lower than that of PBDT [30]. Since the donor of them is same, the decrease of E_g is due to the nitrogen atom in acceptor of PEDOT-PT which increase the ability of withdrawing electron and conjugative effect.

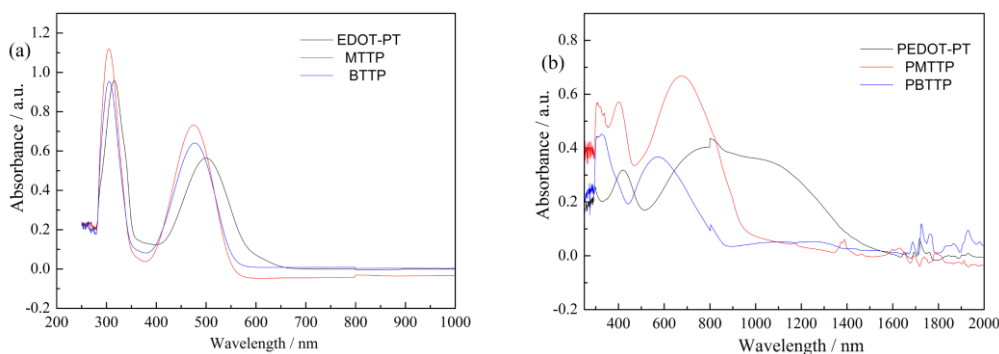


Figure 7. (a) UV-vis absorption spectra of EDOT-PT, MTTP and BTTP monomer in DCM. (b) Absorption spectra of the corresponding polymers deposited on ITO at the neutral state.

Table 1. The onset oxidation potential (E_{onset}), maximum absorption wavelength (λ_{max}), absorption onsets wavelength (λ_{onset}), HOMO and LUMO energy levels and optical band gap (E_g)

Compounds	E_{onset} (V)	λ_{max} (nm)	vs.(Ag- wire) λ_{onset} (nm)	E_g^a (eV)	E_g^d (eV)	HOMO ^b (eV)	LUMO ^c (eV)
EDOT-PT	0.94	315,501	594	2.09	1.982	-5.36	-3.27
MTTP	1.32	305,475	550	2.26	2.245	-5.74	-3.48
BTTP	1.28	305,477	560	2.21	2.238	-5.70	-3.49
PEDOT-PT	0.40	417,771	1458	0.85		-4.82	-3.97
PMTTP	0.97	399,672	949	1.31		-5.39	-4.08
PBTTP	0.95	321,571	848	1.46		-5.37	-3.91
PBDT^e	-	428,755	1043	1.19			

^acalculated from the low energy absorption edges(λ_{onset}), $E_g=1241/\lambda_{\text{onset}}$

^bHOMO = $-e(E_{\text{onset}} + 4.4)$ (E_{onset} vs. SCE).

^ccalculated by the subtraction of the optical band gap from the HOMO level.

^d E_g is calculated based on DFT.

^eData were taken from Ref [35].

To gain more information about the molecular structure and electrical band gap, density functional theory(DFT) calculations were conducted at the Gaussian 05 programs. The ground-state electron density distribution of the highest occupied molecular orbital (HOMO) and lowest unoccupied molecular orbital (LUMO) are illustrated in Fig.8. The values of band gap based on DFT were given in Table 1. These values based on DFT were found lower than the values from experimentally data which

should be caused by many reasons such as solvent effects and the variation in solid state to the gaseous states and so on[24].

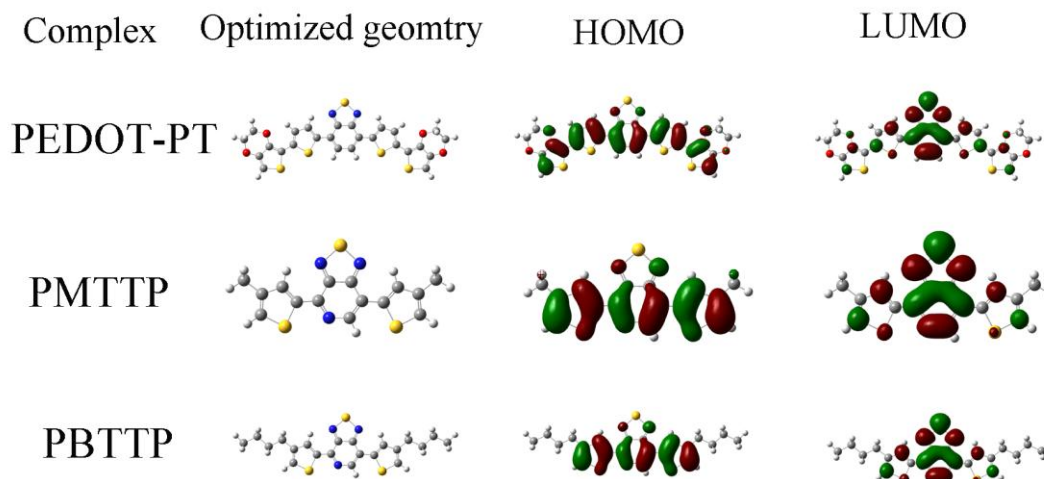


Figure 8. The ground-state electron density distribution of the highest occupied molecular orbital (HOMO) and lowest unoccupied molecular orbital (LUMO) of the three monomers.

3.5. Spectroelectrochemistry of the monomers

Spectroelectrochemistry measurement was conducted for obtaining the information about the $\pi-\pi^*$ electronic transition as a function of the applied potential difference[30]. For the preparation of the working electrode, the polymers were potentiostatically deposited on the ITO electrode in the previously mentioned electrolyte with the same polymerization charge of 2.0×10^{-2} C, and the polymerization potentials are 1.2 V, 1.45V and 1.45 V, respectively, for PEDOT-PT, PMTTP and PBTTP[31]. The in situ UV-vis-NIR spectra of three polymer films were studied upon stepwise oxidation of the polymers in a monomer free electrolyte. Fig.9 reveals the absorption spectra and the colors of PEDOT-PT, PMTTP and PBTTP films, respectively, under different potentials. As can be seen in **Fig.9**, with the enhancement of the gradually applied potentials, the absorption of the two high energy transitions in the visible region diminished, and at the same time, the new bands were appeared and intensified in the near-IR region. The movement of the absorption peak to the near infrared suggested the formation of charge carriers, including polarons and bipolarons[31]. At the neutral state the PEDOT-PT film exhibits blue-green color with absorption peaks at 417 and 771 nm in the visible region and it changes to blue color induced by typical evolution of peak at 1030 nm at the fully oxidized state (Fig.9a). Different from PEDOT-PT, PMTTP film exhibits dark blue color with absorption bands at 399 and 672 nm at the dedoped state, and changes to light blue color with an evolution peaks at 470 and 1337 nm in the fully oxidized state (Fig.9b). The color of PBTTP film changed from bluish violet with absorption peaks at 321 and 571 nm in neutral state to grey with new formed peaks at 477 and 1317 nm in the fully oxidized state (Fig.9c). To our delight, UV-vis spectra for PEDOT-PT and PMTTP (Fig.9a and Fig.9b) display well-defined isosbestic points at approx. 543

nm and 437 nm respectively, indicating that the two polymers were being interconverted between two distinct forms on both occasions: the neutral form and radical cation [31].

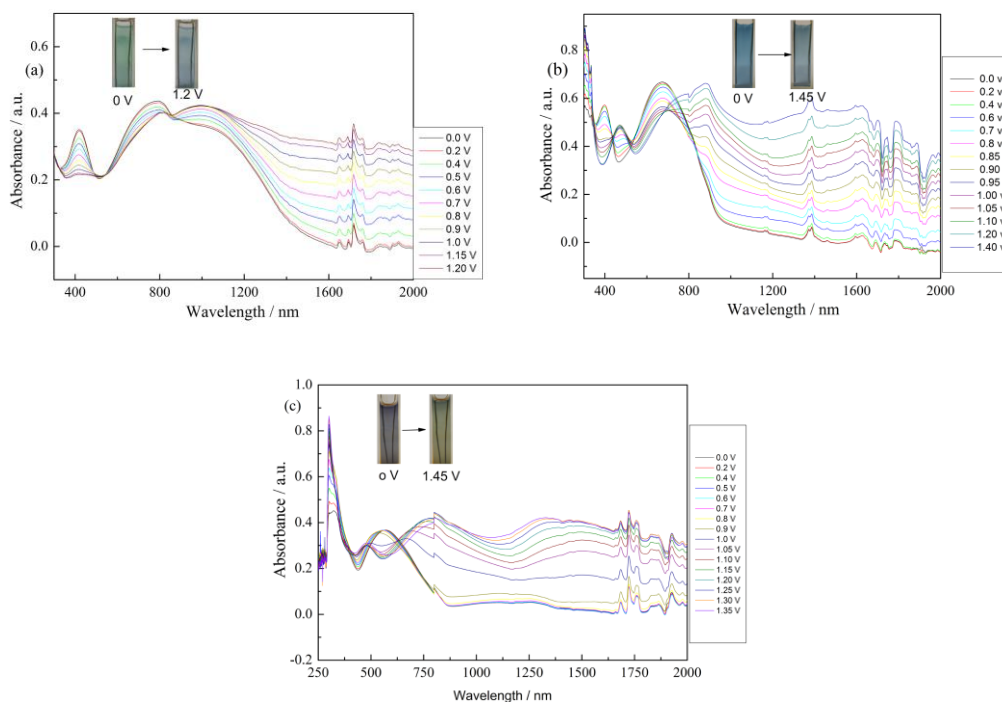


Figure 9. (a) p-doping: Spectroelectrochemistry of PEDOT-PT film on ITO electrode as applied potentials between 0 V and 1.2 V in the monomer-free 0.2 M TBAPF₆/ACN/DCM solution. (b) p-doping: Spectroelectrochemistry of PMTTP film on ITO electrode as applied potentials between 0 V and 1.45 V in the monomer-free 0.2 M TBAPF₆/ACN/DCM solution. (c) p-doping: Spectroelectrochemistry of PBTTT film on ITO electrode as applied potentials between 0 V and 1.35 V in the monomer-free 0.2 M TBAPF₆/ACN/DCM solution.

Table 2. The optical contrasts ($\Delta T\%$), response times and coloration efficiencies (CE) of the PEDOT-PT, PMTTP, PBTTT and PBDT at corresponding wavelengths.

Compounds	λ nm	Optical contrast ($\Delta T\%$)	Response time (s)	Coloration efficiency ($CE \text{ cm}^2\text{C}^{-1}$)
PEDOT-PT	1086	14%	2.17	76.4
	1520	35%	0.63	356.2
PMTTP	395	27%	1.28	100.0
	1307	65%	0.77	140.7
	1506	55%	0.79	156.6
PBTTT	845	18%	1.60	196.7
	1355	62%	1.35	566.3

3.6 Switching properties

The dynamic changes of the absorbance caused by the periodic change of the electric potential are often used to study electrochromic characteristics of the polymer films. The absorption changes at

the dominant wavelengths were recorded as the polymer films were imposed a periodically changed potentials with a switching interval of 4 s. The optical contrast ($\Delta T\%$) is defined as a percent transmittance change at a specified wavelength between the doped and dedoped states [24,32]. The optical contrasts, response time as well as coloration efficiencies of three polymers obtained from the dynamic switching studies at different given wavelengths were summarized in Table 2. Fig. 10 showed the dynamic transmittance changes with the changes of time of the three polymers including PEDOT-PT and PMTTP and PBTTTP. As depicted, the optical contrasts of polymer films in NIR region are relatively satisfactory. The outstanding optical contrast in the NIR region is a very significant property for many NIR applications. Slight losses in percent transmittance contrast value after regular switching during 300 s indicate the high stability of all three films. Beside, we can also notice that the loss of that of PEDOT-PT is the lowest which indicate PEDOT-PT has the best stability. To our surprised, the optical contrast of PMTTP and PBTTTP in visible and NIR region is superior to that of PEDOT-PT. PMTTP film reveals 27% and 65% transmittance changes at 395 nm and 1307 nm between the neutral and oxidized states. As for PBTTTP, they are 18% at 845 nm and 62% at 1355 nm.

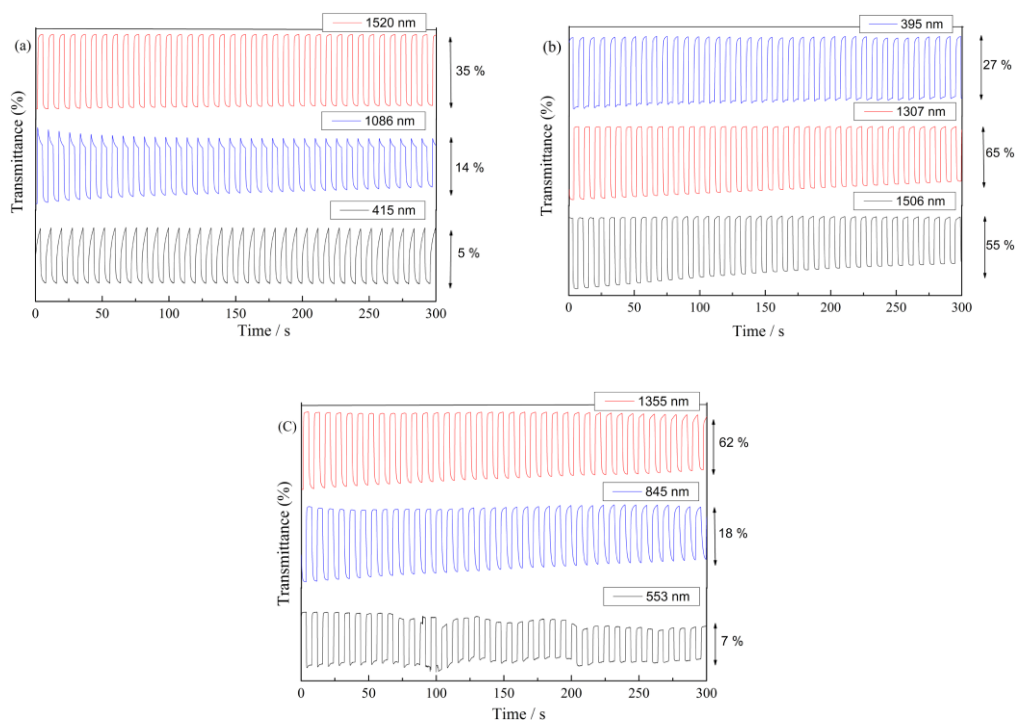


Figure 10. (a) Electrochromic switching, percent transmittance change monitored at 415, 1086 and 1520 nm for PEDOT-PT between 0 and 1.2 V. (b) Electrochromic switching, percent transmittance change monitored at 395, 1307 and 1506 nm for PMTTP between 0 V and 1.45 V.

The appropriated response time is the key to some of the electrochromic devices, such as none emissive display device. Response time is defined as the necessary time for 95% of the full transmittance changes between the neutral and the oxidized states [32]. At the wavelength of 1520 nm, the PEDOT-PT polymer can complete the conversion of the optical contrasts within 0.63 s, which is a

very fast conversion time. For PMTTP, the response times were analyzed to be 1.28 s, 0.77 s and 0.79 s at 395 nm, 1307 nm and 1506 nm, respectively. By contrast, it can be easily found that PEDOT-PT film showed a tiny bit faster switch time in NIR region than that of PMTTP and PBTTP film. The very rapid response processes could be attributable to the rapid counter ion diffusion during the redox process.

The coloration efficiency (CE) is directly related with the power efficiency during the changes in the optical transmittance of the electrochromic materials. CE is the ratio between the change in optical density (ΔOD) and the injected/ejected charge per unit area of the electrode at a specific dominant wavelength (λ_{\max}), and can be illustrated by the following equation[33].

$$\Delta OD = \log \left(\frac{T_b}{T_c} \right) \quad \eta = \frac{\Delta OD}{\Delta Q}$$

Where the T_b is the transmission in the bleached state and T_c is the transmission in the colored state. T_c and T_b values are measured at a nominated wavelength. ΔQ is the charge density, the charge ingress/egress divided by the geometric electrode area of the polymer. CE is expressed in units of $\text{cm}^2 \text{C}^{-1}$ [34]. The CE of PEDOT-PT film was calculated as $356.2 \text{ cm}^2 \text{C}^{-1}$ at 1520 nm and $76.4 \text{ cm}^2 \text{C}^{-1}$ at 1086 nm. The CE values of PMTTP and PBTTP film are summarized in Table 2. As can be seen from Table 2, the CE of PBTTP is $566.3 \text{ cm}^2 \text{C}^{-1}$ at 1355 nm which is enough high to capture our attention[35].

4. CONCLUSIONS

Novel D-A type monomers based on [1,2,5]thiadiazolo[3,4-c]pyridine (PT) as the acceptor unit and EDOT or alkylthiophene as the donor unit were synthesized electrochemically as well as corresponding polymers have been successfully synthesized by electropolymeration. The chemical structure was analyzed with the help of NMR spectra. Electrochemical and spectroelectrochemical characterization demonstrate that PEDOT-PT film with the stronger electron-donor EDOT unit had lower oxidation potentials and lower band gaps. The polymer films showed reversible electrochemical processes and stable color change with high coloration efficiency and optical contrast in INR region when the polymer was switched between the neutral and oxidized states. At the same time, the outstanding optical contrasts in the NIR region, very fast switching times and high environmental stabilities make these polymers paramount choices for electrochromic display applications.

ACKNOWLEDGEMENT

The work was financially supported by the National Natural Science Foundation of China (31400044, 51473074), the General and Special Program of the postdoctoral science foundation China (2013M530397, 2014T70861) and the Natural Science Foundation of Shandong Province (ZR 2014JL009).

Reference

1. C. J. Brabec, N. S. Sariciftci, J. C. Hummelen, *Adv. Funct. Mater.*, 11 (2011) 15.

2. R. J. Mortimer, *Chem. Soc. Rev.*, 26 (1997) 147.
3. N. Stutzmann, R. H. Friend, H. Sirringhaus, *Science.*, 299 (2003) 1881.
4. D. T. McQuade, A. E. Pullen, T. M. Swager, *Chem. Rev.*, 100 (2000) 2537.
5. M. Sendur, A. Balan, D. Baran, B. Karabay, L. Toppare., *Org. Electron.*, 11(2010) 1877.
6. L. Groenendaal, G. Zotti, P.-H. Aubert, S. M. Waybright, J. R. Reynolds, *Adv. Mater.*, 15 (2003) 855.
7. S. A. Sapp, G. A. Sotzing, J. R. Reynolds, *Chem. Mater.*, 10 (1998) 2101.
8. G. E. Gunbas, A. Durmus, L. Toppare, *Adv. Mater.*, 20 (2008) 691.
9. E. E. Havinga, W. Hove, H. Wynbery, *Polymer. Bulletin.*, 29 (1992) 119.
10. E. E. Havinga, W. Hove, H. Wynbery, *Synth. Met.*, 55 (1993) 299.
11. M. Velusamy, K. R. Justin Thomas, J. T. Lin, Y. C. Hsu, K. C. Ho, *Org. Lett.*, 7 (2005) 1899.
12. Y. Cui, Y. Z. Wu, X. F. Lu, X. Zhang, G. Zhou, F. B. Miapah, W. H. Zhu, Z. S. Wang, *Chem. Mater.*, 23 (2011) 4394.
13. D. W. Chang, H. J. Lee, J. H. Kim, S. Y. Park, S. M. Park, L. Dai, J. B. Baek, *Org. Lett.*, 13 (2011) 3880.
14. S. Y. Qu, W. J. Wu, J. L. Hua, C. Kong, Y. T. Long, H. Tian, *J. Phys. Chem. C.*, 114 (2010) 1343.
15. W. J. Ying, J. B. Yang, M. Wielopolski, T. Moehl, J. E. Moser, P. Comte, J. L. Hua, S. M. Zakeeruddin, H. Tian, M. Grätzel, *Chem. Sci.*, 5 (2014) 206.
16. Q. Y. Feng, X. F. Lu, G. Zhou, Z. S. Wang, *Phys. Chem. Chem. Phys.*, 14 (2012) 7993.
17. Y. Sun, G. C. Welch, W. L. Leong, C. J. Takacs, G. C. Bazan, A. J. Heeger, *Nat. Mater.*, 11 (2012) 44.
18. N. Blouin, A. Michaud, D. Gendron, S. Wakim, E. Blair, R. Neagu-Plesu, M. Belletête, G. Durocher, Y. Tao, M. Leclerc, *J. Am. Chem. Soc.*, 130 (2008) 732.
19. Y. Hun, H. D. Wang, X. J. Zhu, A. Islam, L. Y. Han, C. J. Qin, W. Y. Wong, W. K. Wong, *Dyes Pigments.*, 102 (2014) 196.
20. S. Ming, S. Zhen, K. Lin, L. Zhao, J. K. Xu, B. Y. Lu, L. Wang, J. Xiong, Z. Zhu., *J. Electron. Mater.*, 44 (2015) 1606.
21. W. Ying, X. Zhang, X. Li, W. Wu, F. Guo, J. Li, H. Ågren and J. Hua, *Tetrahedron.*, 70 (2014) 3901.
22. D. Arıcan, A. Aktaş, H. Kantekin, A. Koca, *Sol. Energy Mater. Sol. Cells.*, 132 (2015) 289.
23. Q. Hou, Q. Zhou, Y. Zhang, W. Yang, R. Yang, Y. Cao, *Macromolecules.*, 37 (2004) 6299.
24. H. Zhao, Y. Y. Wei, J. S. Zhao, M. Wang, *Electrochim. Acta.*, 146 (2014), 231-241.
25. H. Zhao, D. D. Tang, J. S. Zhao, M. Wang, J. M. Dou, *RSC Advance.*, 4(2014) 61537.
26. B. Y. Lu, C. C. Liu, Y. Z. Li, J. K. Xu, G. D. Liu, *Synthetic Met.*, 1 (2011) 188.
27. F. Algi, A. Cihaner, *Org. Electron.*, 10(2009) 704.
28. S. Celebi, A. Balan, B. Epik, D. Baran, L. Toppare, *Org Electron.*, 10(2009) 631.
29. U. Salzner, M. E. Kose, *J. Phys. Chem. B.*, 106 (2002) 9221.
30. J. Hwang, J. I. Son, Y. B. Shim, *Sol. Energy Mater. Sol. Cells.*, 94 (2010) 1286.
31. Y. X. Liu, M. Wang, J. S. Zhao, C. S. Cui, J. F. Liu, *RSC Advance.*, 4 (2014) 52712.
32. A. Cihaner, F. Algi, *Electrochim. Acta.*, 54 (2008) 786.
33. S. Tarkuc, E. K. Unver, Y. A. Udum, L. Toppare, *Eur. Polym. J.*, 46(2010) 2199.
34. M. Fabretto, T. Vaithianathan, C. Hall, P. Murphy, P. C. Innis, J. Mazurkiewicz, G. G. Wallace., *Electrochem. Commun.*, 9(2007) 2032.
35. D. Baran, G. Oktem, S. Celebi, L. Toppare, *Macromol. Chem. Phys.*, 212 (2011) 799.